

Full-bridge DC-DC Converter based on Linear Active Disturbance Rejection Control

Xuequan Hua

School of Information and Control Engineering, Jilin Institute of Chemical Technology, Jilin Jilin, 132000, China

Abstract: Dual Active Bridge (DAB) converter has been a research hotspot in recent years. It is widely used in distributed power generation system, DC microgrid system and power management system. Traditional PI controllers do not perform well in the face of nonlinear loads and external disturbances, so a more advanced control method is needed to improve the stability and performance of the system. In this paper, a control strategy based on active disturbance rejection control (ADRC) is proposed to improve the control performance of full-bridge DC-DC converter. First of all, the small signal mathematical model of full-bridge DC-DC converter is established, and the function relationship between input, output, control quantity and disturbance quantity in the system is obtained. Then, the extended state observer of ADRC core module is designed, and its parameters are adjusted and simulated, compared with the traditional PI controller. The simulation results show that the full-bridge DC-DC converter based on LADRC has faster dynamic response and better disturbance immunity, which can effectively improve the stability and robustness of the system.

Keywords: Dual Active Bridge DC-DC Converter; Linear Active Disturbance Rejection Control; Robustness.

1. Introduction

The isolated dual active bridge DC-DC (DAB) converter has the advantages of bidirectional power flow, high power density, easy to realize zero voltage switching, convenient for cascade and parallel processing, etc. Therefore, DAB converter plays a connecting role in the system, and its control effect will directly affect all aspects of the energy conversion system. Therefore, DAB has gradually become the research hotspot of bidirectional DC converter, and its immunity and dynamic response control have also attracted the attention of many scholars[1].

There are two ways to improve the performance of switching converters, one is to propose a new circuit topology, the other is to find a better control strategy. The difficulty of improving the converter topology depends on the degree of functionality and performance enhancements required. Simple enhancements, such as efficiency improvements or adaptations of specific input and output voltages, may require only minor adjustments to existing topologies. However, implementing complex features, such as increased isolation, multi-port support, or reduced inductance, often requires in-depth circuit design knowledge and system-level optimization, and can therefore involve greater engineering challenges and cost inputs. Therefore, it is more convenient to optimize the converter from the control strategy. It is very important to realize the immunity and robustness of DAB converter in the complex and dangerous environment such as input voltage fluctuation and output load disturbance. At present, the traditional closed-loop control strategy is PI control, whose control mode is relatively simple and the design is relatively concise. However, due to the defects of the algorithm itself, it is difficult for the DAB converter to quickly recover to the original state under harsh environment (such as large disturbance of input and output, etc.), and the dynamic response is slow, resulting in poor system performance. At present, in addition to the PI controller, the control methods to improve the stability of the system include fuzzy neural network prediction[2], synovium control[3], etc.

Although these methods are better than the traditional PI control, their application is still limited because they rely too much on the parameters and natural frequencies of the control system model.

There are many limitations in power transmission, including input voltage, output voltage, switching frequency of the system, equivalent inductance, shift ratio, etc. However, for a definite DAB converter, its system parameters are fixed, such as input and output voltage, switching frequency, equivalent inductance, etc. And its shift ratio D is a physical quantity that can be adjusted by control. In the traditional closed-loop control mode of DAB converter, PI controller is used to adjust the shift ratio and then control the transmission power of the system. The purpose of the controller designed in this paper is to control the voltage stability of the DC bus, and to achieve stability under various disturbances. In the case of large shift ratio, the initial value of energy will be very large, which is not conducive to the transmission speed of current, resulting in its rising speed too slow, which will limit the transmission power; In the case of small shift ratio, the current will rise rapidly at this time, which will lead to insufficient transmission power, resulting in a waste of energy.

Active Disturbance Rejection Control (ADRC) is a control strategy based on modern control theory, which does not depend on the internal information of the object, and has the advantages of simple structure and strong adaptability. It can solve the contradiction between fast response and overshoot of PI controller, and has the characteristics of good dynamic response and strong anti-interference ability. In 2018, Zhiqiang Gao proposed a linear active disturbance rejection control method (LADRC), which can greatly simplify the tuning of ADRC parameters and provide a good reference for other scholars to study ADRC[4]. Based on the above research, this paper designs a control strategy based on linear active disturbance rejection control (LADRC) for DAB converter and verifies its good control effect through simulation.

2. System Modeling of DAB Converter

2.1. Circuit Topology of DAB Converter

Figure 1 shows the circuit topology structure diagram of DAB converter. Although the number of power switching tubes (active semiconductor fully controlled type) is increased for DAB converter, its control modes are correspondingly increased and the degree of freedom is increased, which is more suitable for the scene with large fluctuation range on input side and load side[5]. When the input voltage changes and load change range is large, by adding the phase shift Angle control between the bridge arms, the return power can be reduced, so as to reduce the loss of the converter, which also does not have much influence on the zero-voltage switch of the switching tube.

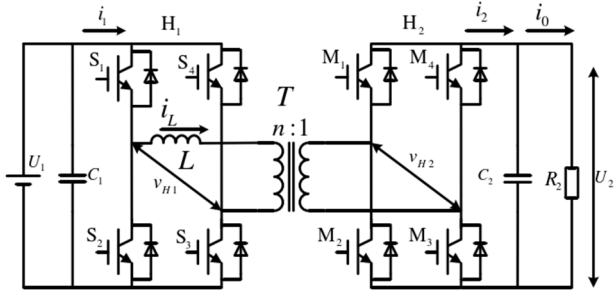


Figure 1. Topology structure of dual active DAB converter

The DAB converter consists of a primary bridge H_1 (S_1 - S_4) and a secondary bridge H_2 (M_1 - M_4) connected by a high-frequency transformer T . L is the transmission inductance; U_1 and U_2 are the DC voltage of the primary side (input voltage) and the secondary side (output voltage) respectively. R_2 is equivalent load of DAB converter; C_1 is the protection capacitor on the input side, and C_2 is the support capacitor on the output side. i_1 , i_2 and i_0 are the input current, output current and load current of the converter respectively, and i_L is the current flowing through the equivalent inductance L . The ratio of the transformer is $K=n:1$.

2.2. Power Analysis of Single Phase Shift Control

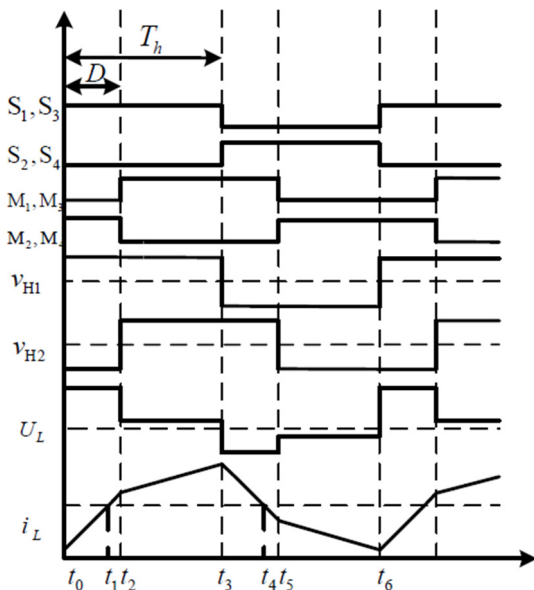


Figure 2. Waveform diagram of steady-state controlled by single phase shift

DAB converter commonly used Single Phase Shift control (SPS), this control mode is easy to achieve, can reduce the voltage and current stress of the power switch tube. The steady-state waveform diagram of single-phase shift control of DAB converter is shown in Figure 2.

In the figure, S_1 - S_4 and M_1 - M_4 are the corresponding switch control signals with the same frequency and duty cycle of 0.5. The diagonal switch control signals are the same and complementary to the other diagonal signal. T_h is half a switching period, $T_f=1/2f$ (f is the switching frequency), T_s is a switching period; D represents the shift ratio between H_1 and H_2 Bridges, i.e. $D=\phi/\pi$; U_L Indicates the voltage at both ends of the inductor. $D>0$ indicates that the power flows from the primary side to the secondary side, that is, the energy passes through positively. $D<0$ indicates that the power flows from the secondary side to the primary side, that is, the energy flows in reverse. Due to the symmetrical structure of DAB converter, the forward flow of energy and the reverse flow mechanism are the same. In this paper, the forward flow of energy is used as the basis for analysis.

By analyzing the steady-state mechanism of DAB converter under single phase shift control, it is not difficult to conclude that the current i_L flowing through the equivalent inductor L is centrosymmetric in one cycle, then the algebraic sum of the inductor current in one cycle is zero, and only the mathematical model of steady-state power in one cycle needs to be calculated.

In one cycle, according to the DAB definition, the transmitted power expression 1 of the DAB converter under SPS control can be obtained as follows:

$$P = \frac{1}{T_s} \int_0^{T_s} v_{H1} i_L dt = \frac{nU_1 U_2}{2fL} D(1-D) \quad (1)$$

Since the conversion circuit of the DAB converter on both sides of the high-frequency transformer is symmetrical, the above analysis method can also obtain the power expression during DAB reverse transmission, so the total power expression of the DAB converter during power expression 2 can be obtained:

$$P = \frac{nU_1 U_2}{2fL} |D|(1-|D|) \quad (2)$$

$D>0$, indicates forward power transmission; $D<0$, reverse power transmission.

According to power expression 2, the relationship between its own variable D and power P can be drawn, as shown in Figure 3.

It can be seen from the figure that when the transmission power transmits energy in the reverse direction, $D \in (-1,0)$, the absolute value of the transmission power first increases and then decreases with the increase of the shift ratio. When $D \in (0,1)$, the power is transmitted forward, and the change of the absolute value of the transmitted power is the same as in the reverse transmission. The transmission power has a maximum of $nU_1 U_2 / 8fL$ if and only if $D = \pm 0.5$.

In the process of energy transmission, if the energy loss of various devices is not considered, it can be considered that the input power of the system is equal to its output power, and the power on the output side can be expressed by the formula $2P_2 = U_2 / R_2$, where R_2 represents the load resistance on the output side. From Formula 1 and the power expression of the output side system can be obtained as follows:

$$U_2 = \frac{nU_1}{2fL} D(1-D)R_2 \quad (3)$$

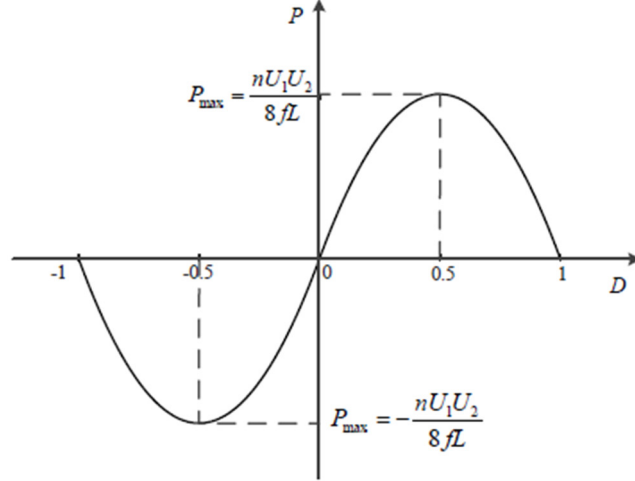


Figure 3. Shift compared to the transmission power graph

Similarly, when the power is transmitted in reverse, the expression 4 of U_1 is:

$$U_1 = \frac{nU_2}{2fL} D(1-D)R_1 \quad (4)$$

Where R_1 is the equivalent load resistance on the U_1 side.

If the average value of input and output current is multiplied by the equivalent resistance of each side to represent the power of each side, the expression 5 of the average value of the current of each side can be obtained:

$$\begin{cases} I_1 = \frac{nU_2}{2fL} D(1-D) \\ I_2 = \frac{nU_1}{2fL} D(1-D) \end{cases} \quad (5)$$

2.3. DAB Small Signal Modeling and its Design Accuracy

The small-signal modeling of DAB converter is the basis for analyzing the closed-loop control and parameter design of the converter, because we can deduce the transfer function of DAB converter from the small-signal model, which is of great help to the parameter design of the control of DAB converter.

According to expression 5, the average physical model of DAB can be obtained. By adding small disturbance signals to the steady-state model of DAB converter, and then separating the disturbance and ignoring the quadratic term, the first-order small signal model of DAB converter can be obtained, and then the corresponding closed-loop control design can be carried out. In order to introduce low frequency small signal disturbance, perturbation $U_1 \rightarrow U_1 + \hat{u}_1$, $U_2 \rightarrow U_2 + \hat{u}_2$, $I_1 \rightarrow I_1 + \hat{i}_1$, $I_2 \rightarrow I_2 + \hat{i}_2$, $D \rightarrow D + \hat{d}$ is added to the input current, output current and shift ratio expression obtained by equation 5, By eliminating the direct flow and high-order disturbance existing in the formula, the following expression 6 can be obtained:

$$\begin{cases} \hat{i}_1 = b_1 \hat{d} + b_2 \hat{u}_2 \\ \hat{i}_2 = b_3 \hat{d} + b_2 \hat{u}_1 \end{cases} \quad (6)$$

In Formula 6, $b_1 = nU_2(1-2D)/2fL$, $b_2 = nD(1-D)/2fL$, $b_3 = nU_1(1-2D)/2fL$.

Thus, DAB small signal model can be obtained, as shown in Figure 4:

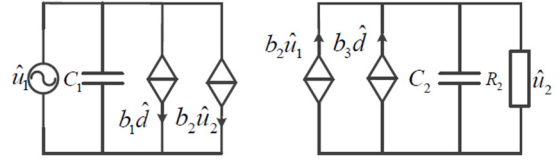


Figure 4. Small signal model of DAB

From Figure 4, the transfer function formula 7 of DAB control quantity to output can be obtained:

$$G_{u_2 d} = \frac{\hat{u}_2}{\hat{d}} \Big|_{\hat{u}_1=0} = \frac{b_3 R_2}{R_2 C_2 s + 1} \quad (7)$$

Formula 7 represents the effect on the voltage on the load side when the shift ratio of the system is disturbed.

Some parameters of the system in this paper are: $U_1=400V$, $U_2=100V$, $L=150\mu F$, $C_1=C_2=500\mu F$, $R_2=2\Omega$, $f=20kHz$. According to formula 3, the shift ratio $D=1/4$ of the system in the steady state can be obtained. According to Equation 7 and substituting relevant data, the initial open-loop transfer function 8 of the system without using PI controller can be obtained as follows:

$$G_{op} = \frac{266.667}{0.001s+1} \quad (8)$$

The Bode diagram of the transfer function of the system can be made by MATLAB software, and the Bode diagram of the model can be obtained by small signal modeling method, as shown in Figure 5 below:

It is proved that the establishment of the above physical model is relatively accurate, which is consistent with the previous theoretical analysis. It can be seen from the figure that the system is stable, but it can also be seen that the gain of the system in the low frequency band is low, and there is a certain steady-state error, so the system needs to be corrected.

3. Controller Design

It can be seen from formula 7 that the system can be simplified into a first-order system, so a first-order active disturbance rejection controller is designed. According to Equation 7 and the small signal model in Figure 4, the time-domain expression of DAB expression 9 can be written:

$$C_2 \frac{d\hat{u}_2}{dt} = \frac{nU_1(1-2D)}{2fL} \hat{d} - \frac{\hat{u}_2}{R_2} \quad (9)$$

Formula 9 can be written as the general form 10 as follows:

$$\dot{y} = -a_1 y + w + bu \quad (10)$$

The controller is designed to maintain the stability of the

output voltage. The control quantity is shifting ratio D , y represents the output voltage of the transformer, and the output U of the controller represents shift ratio D . w represents the disturbance in the internal and external parts of

the system, and a_1 is the internal parameter of the DAB converter (a_1 and w are unknown). If b is the input control gain and part of it is known (known part is b_0 , $b_0 = nU_1(1-2D)/2fL$), then the above formula can be written as 11:

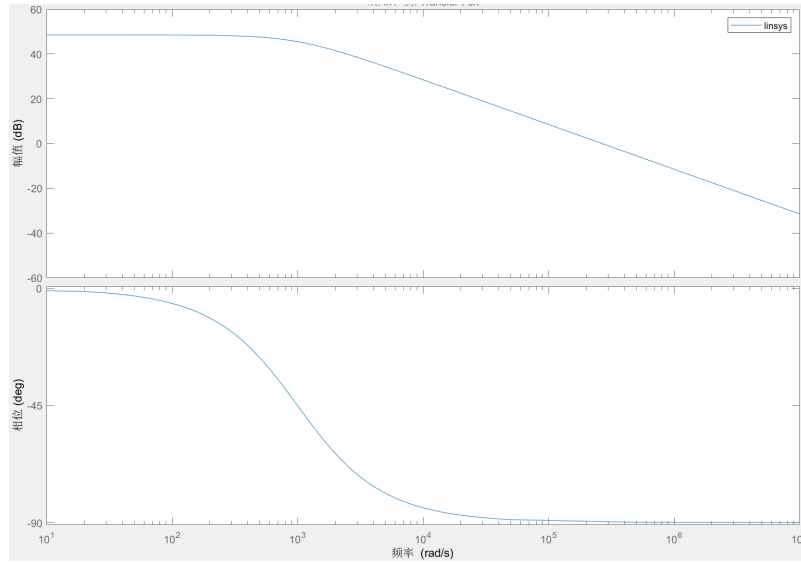


Figure 5. Bode diagram of the open-loop transfer function of the system before adding the controller

$$\dot{y} = -a_1 y + w + (b - b_0 u) + b_0 u = f + b_0 u \quad (11)$$

Choose state variables $x_1=y, x_2=f$, and let $h = \dot{f}(y, w)$ to obtain the equation of state of the expression 12:

$$\begin{cases} \dot{x}_1 = x_2 + b_0 u \\ \dot{x}_2 = h \\ y = x_1 \end{cases} \quad (12)$$

Equation of expression 13 for establishing LESO is as follows:

$$\begin{cases} \dot{z}_1 = z_2 - \beta_1(z_1 - y) + b_0 u \\ \dot{z}_2 = -\beta_2(z_1 - y) \end{cases} \quad (13)$$

In the formula, Z_1 and Z_2 are state variables of LESO; β_1 and β_2 are observer gain parameters. $z_1 \rightarrow x_1, z_2 \rightarrow x_2$, where h is unknown, but can be estimated by LESO, so it can generally be ignored in LESO equation of state description. If the parameters are selected reasonably, the LESO state variables can track the system state variables in real time.

The first-order linear error state feedback law (LESF) is 14 because it does not need to observe the differential signal of the system state variable:

$$u_0 = k_p(v - z_1) \quad (14)$$

In the formula, U_0 represents the output item of LESF, and K_p represents the gain of the proportional controller.

The traditional PI controller can eliminate the error of the system through integration, which will reduce the stability of the system. The first-order LADRC can make use of second-order LESO to compensate the generalized disturbance in real time, which can effectively avoid the influence of the integral link [6]. The total disturbance of the system is estimated by expanding the state variables, and the input of the system is compensated. Formula 15:

$$u = \frac{(-z_2 + u_0)}{b_0} \quad (15)$$

If the error of Z_2 's estimation of the total disturbance is ignored, then substituting equation 14 into equation 11 can be simplified to an integral component equation 16:

$$\dot{y} = (f(y, w) - z_2) + u_0 \approx u_0 \quad (16)$$

According to equations 13 and 15, the closed-loop transfer function 17 of the DAB converter can be sorted out as follows:

$$\varphi(s) = \frac{k_p}{s+k_p} = \frac{1}{1/k_p \cdot s + 1} \quad (17)$$

As can be seen from equation 17, the bandwidth of LSEF $\omega_c = k_p$, so in order to make the system eventually stable, to choose a better proportional gain value [7]. The detailed internal control structure diagram of LADRC of the system can be obtained according to formula 10, 13 and 14, as shown in Figure 6:

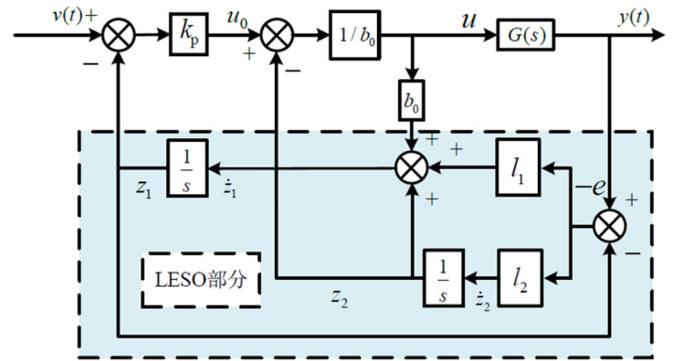


Figure 6. Detailed internal structure of first-order LADRC

In order to further simplify the parameter design of the state observer, the gain matrix of the observer is associated with the bandwidth of the observer through the method of pole parameter configuration, and the pole of equation 13 is assigned to the bandwidth w_0 of LESO, namely, equations 18 and 19:

$$\lambda(s) = s^2 + l_1 s + l_2 = (s + \omega_0)^2 \quad (18)$$

$$\begin{cases} l_1 = 2\omega_0 \\ l_2 = \omega_0^2 \end{cases} \quad (19)$$

After the above mathematical analysis, the parameters of the ladrc can be found to be properly configured with two parameters, and ω_c, ω_0 is able to make the control effect of the controller achieve the desired state [8].

4. Control Effect Verification

In order to verify the superiority of the proposed LADRC

control strategy, the control simulation model of DAB converter is built based on MATLAB/Simulink simulation software. It is compared with the traditional PI single closed loop control. The internal parameters of DAB converter are shown in Table 1, and the controller parameters are shown in Table 2:

Table 1. Detailed parameters of DAB converter

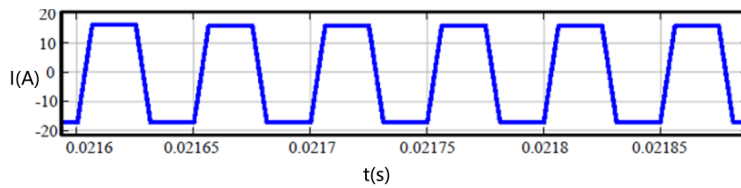
| Argument | Numerical value | Unit |
|----------------------|-----------------|-------------|
| Supply voltage | 400 | U_1/V |
| Output voltage | 100 | U_2/V |
| Ratio of transformer | 4:1 | n |
| Switching frequency | 20 | f/kHz |
| Series inductance | 150 | L/ μH |
| Input capacitance | 500 | $C_1/\mu F$ |
| Output capacitance | 500 | $C_1/\mu F$ |

Table 2. Controller parameters

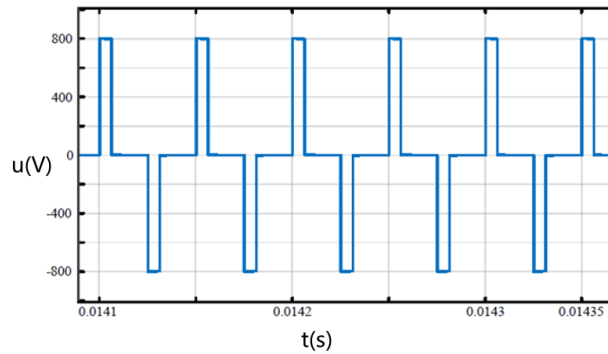
| Argument | Numerical value |
|---------------------------------|-----------------|
| Observer bandwidth ω_0 | 1200 |
| Controller bandwidth ω_c | 10000 |
| Control gain b_0 | 100000 |

In the process of parameter setting in this paper, the size of b_0 is first determined, w_c remains unchanged, and w_0 is gradually increased until the impact of noise meets the requirements of the system. Then gradually increase w_c , reduce w_0 when the system cannot withstand the noise, and then increase w_c , when the ideal waveform curve is basically reached, then fine-tune ω_0 and ω_c until the expected effect is better.

The simulation model of the system was built in simulink simulation software. When the system reached a steady state, the main working waveform was shown in Figure 7.



(a) Inductive current waveform



(b) inductance voltage waveform

Figure 7. Working waveform of stable working system

According to (a) and (b) in FIG. 7, it can be seen that the voltage and current at both ends of the inductor are consistent with the final result of phase shift control analyzed above. Therefore, the final control effect of the LADRC strategy proposed in this paper is consistent with the results of the previous mathematical analysis, which can realize the control of DAB converter.

In order to verify the good immunity of LADRC compared with PIDE, this paper tests the superiority of the control strategy by adding disturbance on the load side and power supply.

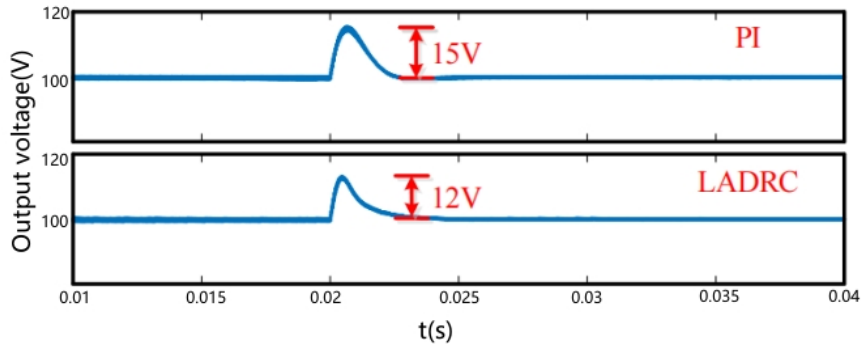
(1) Load mutation

Figure 8 compares the dynamic response of the two control schemes with a step change in load ($2\Omega-4\Omega-2\Omega$). It can be seen from FIG. 8 (a) that when the load of the DAB converter suddenly increases at 0.02s, the output voltage returns increases to a certain extent, and then returns to the initial state after a short process. In FIG. 8 (b), when the load of the system suddenly decreases at 0.05s, the output voltage return of the DAB converter decreases instantaneously and also returns to the original state. This shows that the closed-loop design of the two control schemes of DAB transformation

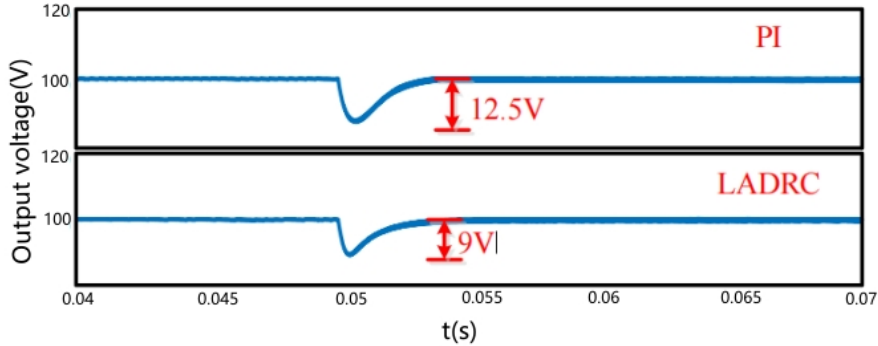
meets the dynamic response requirements of the system and has a certain anti-disturbance ability. As can be seen from Figure 8, the dynamic response of LADRC strategy is much better than that of PI control scheme no matter the load increases or the load decreases. In LADRC control scheme, when the load increases, the adjustment time is shortened by 2ms compared with PI control, and the overshoot is reduced to 3V compared with PI control, and the overshoot time and overshoot also change significantly when the load decreases. Therefore, the LADRC control scheme can significantly improve the dynamic response and robustness of the system.

(2) Input voltage mutation

Figure 9 (a) shows the output voltage waveform when the input voltage suddenly decreases from 400V to 350V, and Figure 9 (b) shows the voltage waveform when it recovers to 400V. It can be clearly seen from Figure 9 that the overshoot of LADRC during the transition process of restoring to the initial value when the input voltage suddenly increases or decreases, is about twice the overshoot of PI control strategy. The transition time is significantly faster than PI control. Therefore, the anti-input voltage disturbance capability of LADRC is better than that of PI control strategy.

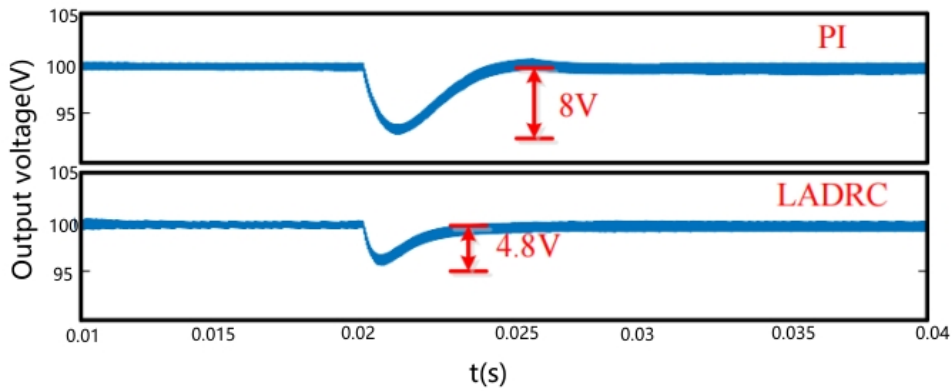


(a) Sudden increase in load

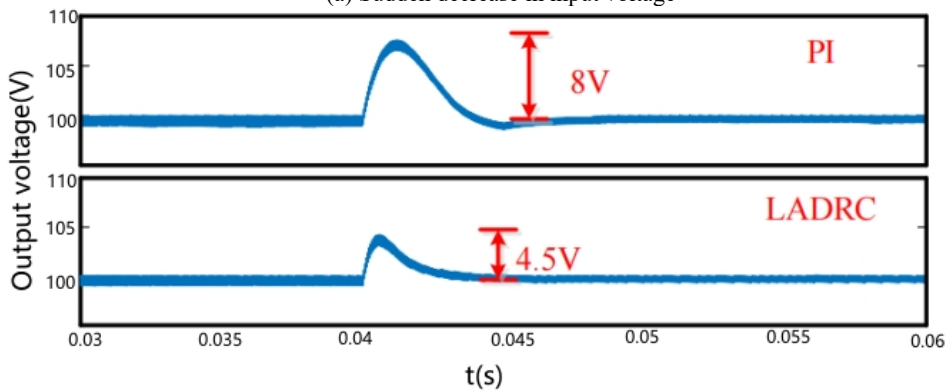


(b) Sudden load reduction

Figure 8. Load mutation



(a) Sudden decrease in input voltage



(b) The input voltage is restored to 400V

Figure 9. Input voltage

5. Summary

In order to improve the dynamic response and immunity of DAB converter, the working principle of DAB converter is analyzed first, and then small signal modeling is carried out. On this basis, an active disturbance rejection controller based on LESO is designed. The anti-interference ability of this

control strategy is significantly better than that of PI control in the face of load side disturbance and power side disturbance. Therefore, the control strategy proposed in this paper has a good application prospect in the control of DC/DC converter.

References

- [1] Hou Nie, Li Yunwei. Overview and comparison of modulation and control strategies for non-resonant single-phase dualactive-bridge DC-DC converter[J]. IEEE Transactions on Power Electronics, 2019,35(3):3148-3172.
- [2] HEDLUND M, OLIVEIRA J G, BERNHOFF H. Sliding mode 4-quadrant DCDC converter for a fly-wheel application[J]. Control Engineering Practice, 2013, 21(4): 473-482.
- [3] CHEN Q, REN X M, OLIVER J A. Identifier-based adaptive neural dynamic surface control for uncertain DC-DC buck converter system with input constraint[J]. Communications in Nonlinear Science and Numerical Simulation, 2012, 17 (4): 1871-1883.
- [4] Gao Zhiqiang. Scaling and bandwidth-parameterization based controller tuning[C]. Proceedings of the 2003 American Control Conference. Denver: IEEE, 2006:4989-4996.
- [5] Avdeev Boris, Vyngra Aleksei, Chernyi Sergei. Improving the Electricity Quality by Means of a Single-Phase Solid-State Transformer[J]. Designs, 2020, 4(3): 35-35.
- [6] Han J. From PID to Active Disturbance Rejection Control[J]. IEEE Transactions on Industrial Electronics, 2009, 56(3): 900-906.
- [7] Lu Y, Cheng K, Ho S L. Auto-disturbance-rejection control for phase-shifted resonant converter[J]. IEE Proceedings – Electric Power Applications, 2006, 153(5): 711-718.
- [8] Gao Z. Scaling and parameterization based controller tuning [C]// Proceeding of the 2003 American Control Conference. IEEE, 2003: 4989-4996.